

## Influence of silicon in low density Fe-C-Mn-Al Steel

Yoon-Uk Heo<sup>a</sup>, You-Young Song<sup>a</sup>, Seong-Jun Park<sup>b</sup>, H. K. D. H. Bhadeshia<sup>a,c</sup>, Dong-Woo Suh<sup>a</sup>

<sup>a</sup>Graduate Institute of Ferrous Technology, POSTECH, Pohang 790-784, Korea

<sup>b</sup>Korea Institute of Materials Science, Changwon, 641-010, Korea

<sup>c</sup>Materials Science and Metallurgy, University of Cambridge, CB2 3QZ, U.K.

---

### Abstract

The influence of silicon on the microstructure of a Fe-Mn-Al-C ferritic low-density steel is investigated. The formation of  $\kappa$ -carbide, known to be detrimental to ductility, can be suppressed by reducing the aluminum content to 5 wt.pct. However, the attempt to compensate the light-weighting effect of aluminum by silicon is not desirable because the precipitation of  $(\text{Fe,Mn})_5(\text{Si,Al})\text{C}$  and  $(\text{Fe, Mn})_3(\text{Al, Si})\text{DO}_3$  ordered phase in ferrite grains leads to a serious deterioration in ductility.

*Keywords:* low-density steel, microstructure, silicon, ductility, carbide

---

The FeMnAlC system has been actively researched over many decades for cryogenic applications, for oxidation resistance when the aluminum concentration is large, and in the context of substitution of more expensive stainless steels [1–5]. The subject has been reviewed with key papers beginning in the late 1950s [6]. The present work focuses on an emerging demand for steels of low density. In contrast to the conventional high-strength steels where the components can be made lighter by reducing section-thickness, low-density steels can achieve the same goal through a reduction in density [7–13]. Light elements such as aluminum can be added to steel for that purpose. It is known that approximately 8 wt.pct. Al in steel leads to a reduction in density of 10% [7].

Low-density steels based on Fe-Mn-Al-C system in which the matrix phase can be either ferrite or austenite depending on the content of carbon and manganese have been actively investigated [7–9, 11–15]. Among them, ferritic

---

*Email address:* dongwoo1@postech.ac.kr (Dong-Woo Suh)

low-density steels containing low carbon, medium manganese of 6–8 wt. pct. have attracted attention because greater concentrations of manganese increase the cost of production [12, 13]. However, the ferritic low-density steel has been found to suffer from the loss of ductility with an increase of aluminum content to 6–8 wt. pct., due to the precipitation of  $\kappa$ -carbide that provides vulnerable sites for cracking during deformation [12, 13]. To avoid this deterioration in ductility, an alternative approach might be to reduce the aluminum content marginally to suppress  $\kappa$ -carbide while maintaining the density by exploiting light elements other than aluminum. With this goal in mind, we examine here the evolution of microstructure in a series of ferritic low-density steels where aluminum is substituted partially by silicon.

The investigated alloys are based on Fe-0.2C-8Mn-5Al with 0, 1 or 2 wt. pct. addition of silicon as shown in Table 1. Vacuum-melted ingots were austenitized at 1473K for 1 h followed by hot-rolling with a finishing rolling-temperature above 1243K. The hot-rolled sheets were held for 1 h at 923K for simulating a coiling process and then air-cooled. The microstructure was examined using a field-emission scanning electron microscope (SEM). The precipitates were also investigated in detail using a transmission electron microscope (TEM), the specimens for which were prepared by electro-polishing in a solution of 10 % perchloric acid + 90 % acetic acid at room temperature. As a final polishing step, ion milling was carried out using a precision ion-polishing system. Carbon extraction replica specimens were also prepared to analyze the precipitates. The tensile behavior of hot-rolled sheets was tested with sub-sized specimens according to ASTM E8M at a crosshead speed of 2 mm/min with a gauge length of 25 mm.

Table 1: Chemical composition of the investigated alloys (wt. pct.)

	C	Mn	Si	Al
A	0.23	8.1	-	5.3
B	0.20	8.4	1.0	5.6
C	0.24	8.1	1.8	5.3

Typical microstructures of the alloys are shown in Fig. 1, consisting of alternating layers of elongated ferrite and other layers populated by precipitates. This layered structure evolves through the hot-rolling of a mixture of ferrite and austenite, followed by decomposition of the latter into ferrite

and carbide during cooling. All alloys exhibit similar microstructure in SEM images. Fig. 2 (a) is from alloy A, showing many precipitates of 0.5–1  $\mu\text{m}$  in size observed in annular dark field scanning TEM (STEM) image. The electron diffraction pattern indicated that the precipitates are orthorhombic  $\text{M}_3\text{C}$  carbides ( $a=5.07 \text{ \AA}$ ,  $b=6.75 \text{ \AA}$ ,  $c=4.52 \text{ \AA}$ , ICSD No. 52265). Energy dispersive spectroscopy (Fig. 2(b)) confirms they are  $(\text{Fe,Mn})_3\text{C}$  cementite not containing aluminum. These results indicate that aluminum up to 5 wt. pct. can be tolerated without stimulating the precipitation of  $\kappa$ -carbide in the alloy system examined here.

In Fig. 2(c), which is from alloy B, there are two types of precipitates identified, located within the precipitate-rich layer and at ferrite grain boundaries. Diffraction and microanalysis (Figs. 2(d)–(f)) show that the precipitate marked “1” is orthorhombic  $(\text{Fe,Mn})_5(\text{Si,Al})\text{C}$  ( $a=10.1 \text{ \AA}$ ,  $b=7.99 \text{ \AA}$ ,  $c=7.54 \text{ \AA}$ , ICSD No. 51304) and that marked “2” is  $\kappa$ -carbide with a  $\text{L}_{12}$  structure ( $(\text{Fe,Mn})_3\text{AlC}$ ,  $a=3.857 \text{ \AA}$ ). It is notable that  $\kappa$ -carbide does not contain silicon. Given that the fraction of  $\kappa$ -carbide is relatively small, the addition of 1 wt. pct. Si is thought to convert the major carbide  $\text{M}_3\text{C}$  into  $\text{M}_5(\text{Si,Al})\text{C}$  type. This may be a consequence of the well-known suppression of cementite by silicon addition reported in low carbon steels [16]. The influence of silicon addition is also confirmed in alloy C containing 2 wt. pct. Si as shown in Figs. 3 (a) and (b). The  $\kappa$ -carbide is not observed in alloy C. Furthermore, it is noted that the a silicon addition affects not only the type of carbide but also the microstructure within ferrite. Figs. 3(c) and (d) are from the ferrite grain in alloy C. Minute particles are seen in the ferrite matrix and the electron diffraction (Fig 3(e)) indicates that they are  $\text{DO}_3$  type ordered phase. The microanalysis shown in Fig. 3(f) suggests that the particles with  $\text{DO}_3$  structure are  $(\text{Fe, Mn})_3(\text{Al, Si})$  where aluminum and iron are partially substituted with silicon and manganese, respectively. The precipitation of  $\text{DO}_3$  type ordered phase has been reported in Fe-Al [17–20], Fe-Si [17, 21–23], and Fe-Al-Si [17, 18] alloys. The concentration of 10.1 at% Al and 3.3 at% Si in alloy C is far lower than the minimum for the formation of  $\text{DO}_3$  phase in the binary system, which is known as 20 at% Al [18] or 12 at% Si [21]. However, Miyazaki and coworkers [17] showed the  $\text{DO}_3$  phase could form at lower concentration when aluminum and silicon coexist in the Fe-Al-Si ternary phase. According to their results, at least 10 at% Al and 5 at% Si is needed for the precipitation of  $\text{DO}_3$  in the ferrite matrix at 550°C but the necessary silicon concentration for  $\text{DO}_3$  precipitation is reduced to 3 at% Si at 650°C. Given that the hot-rolled sheet was held for 1 h at 923K,

alloy C possibly had sufficient time for precipitation of fine  $\text{DO}_3$  in ferrite matrix.

Fig. 4 (a) shows the tensile properties of investigated alloys. Compared to the total elongation over 15% in alloy A with tensile strength over 1GPa, that of alloy B is greatly reduced to 5% elongation with negligible elongation exhibited by alloy C. This implies that the precipitation of  $\kappa$ -carbide is avoided and good ductility is secured by reducing the aluminum content to 5 wt. pct., but an addition of silicon is detrimental to the ductility in ferritic low-density steel. Figs. 4 (b) and (c) represent the fracture surfaces of tensile specimens from alloys B and C. One can distinguish the ferrite layer marked as 1 and the secondary layer populated with  $\text{M}_5(\text{Si,Al})\text{C}$  marked as 2 on the fracture surface in Fig. 4(c). For both of alloys B and C, it is difficult to observe the dimple pattern of ductile fracture. Even with some controversies on the embrittlement effect of silicon in solid solution [24, 25], the silicon up to 2 wt. pct. in solid solution will not have harmful influence in terms of the tensile property. In the present study, however, the addition of 1 wt. pct. Si changes the type of carbide from cementite to  $\text{M}_5(\text{Si,Al})\text{C}$ . This suggests that the precipitation of  $\text{M}_5(\text{Si,Al})\text{C}$  carbide is harmful to the ductility which becomes worse as the content of silicon increases to 2 wt. pct. It is noted that the ferrite layer in alloy C shows cleavage fracture. Indeed, the micro Vickers hardness of ferrite layers is evaluated to be 241, 272 and 413 for alloys A, B, C, respectively. The hardness increase of 31 in alloy B, which is roughly equivalent to an increment of 100 MPa in yield strength, is consistent with solid solution hardening due to silicon, given that 1 wt. pct. Si increases the strength by 83 MPa [26]. The drastic increase of hardness in alloy C indicates that the fine  $\text{DO}_3$   $(\text{Fe, Mn})_3(\text{Al, Si})$  ordered phase significantly hardens the ferrite, which is likely to cause the brittleness. It is reported that the plastic deformation of  $\text{DO}_3$   $\text{Fe}_3\text{Al}$  [27] and  $\text{Fe}_3\text{Si}$  [28] phase is difficult and the precipitation of ordered phase in a specific crystallographic plane of matrix ferrite will induce cleavage fracture with little elongation.

In summary, the formation of  $\kappa$ -carbide which is notorious for the loss of ductility in ferritic low-density steels can be suppressed by maintaining an aluminum content at 5 wt. pct. However, further light-weighting using silicon is not desirable because the change of carbide type from cementite to  $\text{M}_5(\text{Si,Al})\text{C}$  and the formation of  $(\text{Fe, Mn})_3(\text{Al, Si})$   $\text{DO}_3$  ordered phase in ferrite grains seriously compromise the ductility.

[1] G. L. Kayak: Metal Science and Heat Treatment, 1969, vol.11, pp. 95–

97.

- [2] P. Y. Lee, C. S. Chiu, Y. J. Gau and J. K. Wu: High Temp. Mater. and Process, 1992, vol.10, pp. 141–144.
- [3] S. T. Shih, C. Y. Tai and T. P. Perng: Corrosion, 1993, vol.49, pp. 130–134.
- [4] X. M. Zhu and Y. S. Zhang: Corrosion, 1999, vol.54, pp. 3–12.
- [5] A. S. Hamada and L. P. Karjalainen: Canadian Metall. Quaterly, 2006, vol.45, pp. 41–48.
- [6] I. Kalashnikov, O. Acselrad, A. Shalkevich and L. C. Pereira: J. Mat. Eng. and Performance, 2000, vol.9, pp. 597–602.
- [7] G. Frommeyer, U. Brüx: Steel Research Int., 2006, vol.77, pp.627–633.
- [8] U. Brüx, G. Frommeyer, J. Jimenez: Steel Research, 2002, vol.73, pp.543–548.
- [9] R. A. Howell, D. C. van Aken: Iron and Steel Technology, 2009, vol.6, pp.193–212.
- [10] R. G. Baligheid, A. Radharishna: Mater. Sci. Eng., 2001, vol.A308, pp.136–142.
- [11] K. T. Park, G. Kim, S. K. Kim, S. W. Lee, S. W. Hwang, C. S. Lee: Met. Mater. Int., 2010, vol.16, pp.1–6.
- [12] S. Y. Shin, H. Lee, S. Y. Han, C. H. Seo, K. Choi, S. Lee, N. J. Kim, J. H. Kwak, K. G. Chin: Metal. Mater. Trans. A, 2010, vol.41A, pp.138–148.
- [13] S. Y. Han, S. Y. Shin, S. Lee, N. J. Kim, J. H. Kwak, K. G. Chin: Metal. Mater. Trans. A, 2011, vol.42A, pp.138–146.
- [14] S. C. Chang, Y. H. Hsiau and M. T. Jahn: J. Mat. Sci., 1989, vol.24, pp. 1117–1120.
- [15] T. Sahraoui, M. Hadji and M. Yahi: Mat. Sci. and Eng., 2009, vol.523, pp. 271–276.

- [16] E. Kozeschnik, H. K. D. H. Bhadeshia: *Mat. Sci. Tech.*, 2008, vol.24, pp.343–347.
- [17] T. Miyazaki, T. Kozakai, T. Tsuzuki: *J. Mater. Sci.*, 1986, vol.21, pp.2557–2564.
- [18] D. G. Morris, S. Gunther: *Acta Mater.*, 1996, vol.44, pp.2847–2859.
- [19] S. M. Allen: *Phil. Mag.*, 1977, vol.36, pp.181–192.
- [20] M. Palm: *Intermetallics*, 2005, vol.13, pp.1286–1295.
- [21] J. H. Yu, J. S. Shin, J. S. Bae, Z. H. Lee, T. D. Lee, H. M. Lee, E. J. Lavernia: *Mat. Sci. Eng.*, 2001, vol.307, pp.29–34.
- [22] A. Gemperle: *Trans. Met. Soc. AIME*, 1968, vol.242, pp.2287–2294.
- [23] Y. Ustinovshikov, I. Sapagina: *J. Mater. Sci.*, 2004, vol.39, pp.1007–1016.
- [24] R. G. Davies: *Metall. Trans. A.*, 1979, vol.10A, pp.113–118.
- [25] B. Mintz: *Mat. Sci. Tech.*, 2000, vol.16, pp.1282–1286.
- [26] T. Gladman: *The physical metallurgy of microalloyed steels*, Maney, London, UK, 2002
- [27] L. Qiao, X. Mao: *Met. Mater. Trans. A*, 1996, vol.27A, pp.3949–3956.
- [28] S. K. Ehlers, M. G. Mendiratta: *J. Mater. Sci.*, 1984, vol.19, pp.2203–2210.

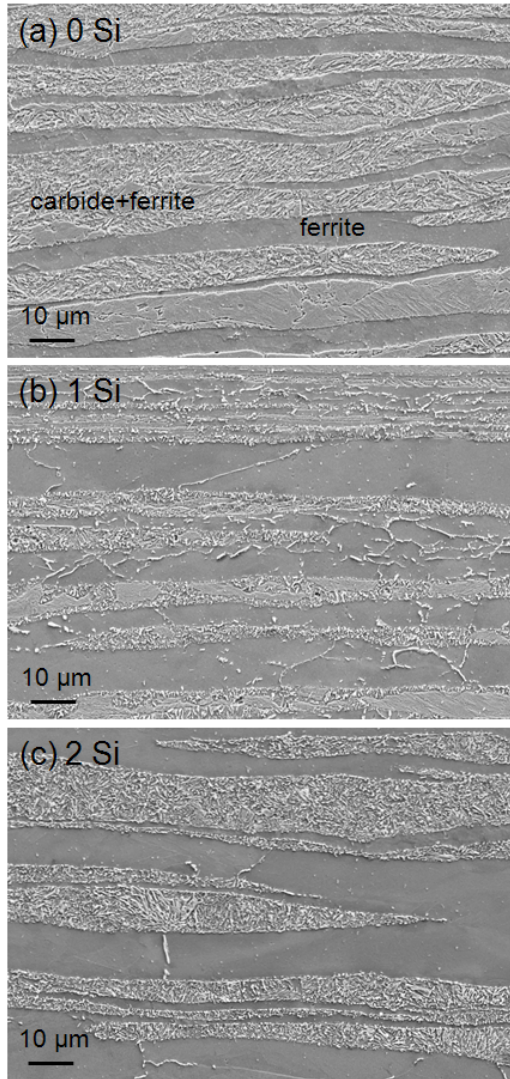


Figure 1: Micrographs of 0.2C-8Mn-5Al alloy with (a) 0 Si, (b) 1 Si and(c) 2 Si in wt. pct.

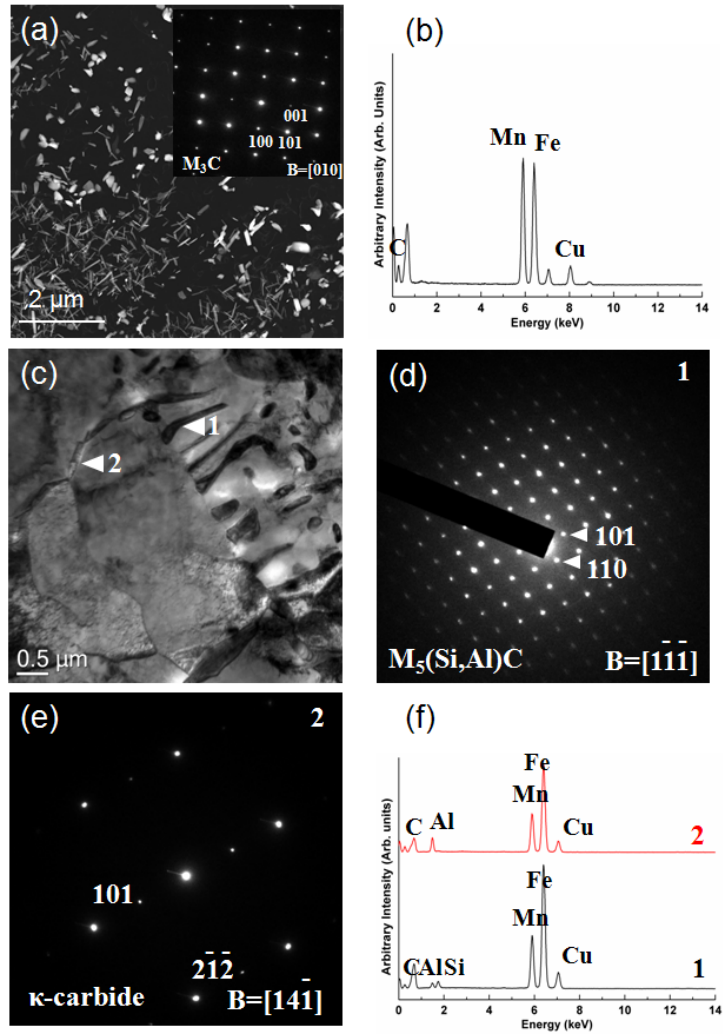


Figure 2: (a) Angular dark field image of alloy a with electron diffraction pattern, (b) Energy dispersive spectroscopy of precipitation in alloy A, (c) Bright field image of alloy B, (d,e) Diffraction pattern from precipitates marked as 1 and 2, (f) Microanalysis from precipitates 1 and 2



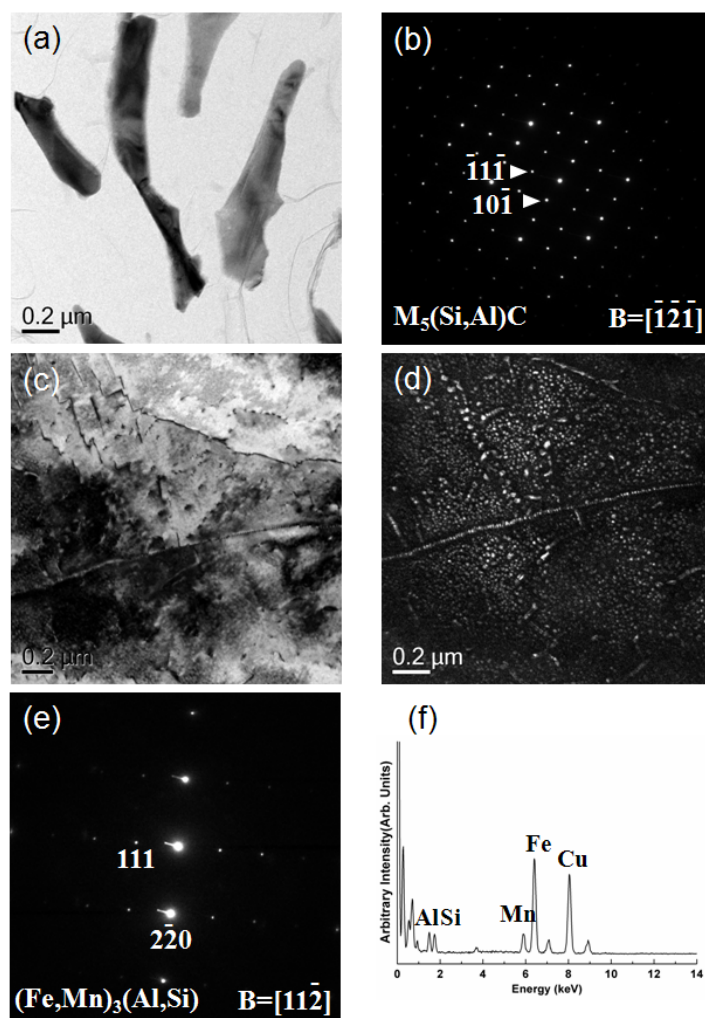


Figure 3: (a) carbon extracted precipitates in alloy C, (b) Electron diffraction pattern from precipitate, (c,d) Bright field and dark field image of ferrite grain, (e) Diffraction pattern from ferrite grain in (c) (spots from  $D0_3$  precipitates are indexed), (f) Energy dispersive spectroscopy of carbon extracted  $D0_3$  precipitate

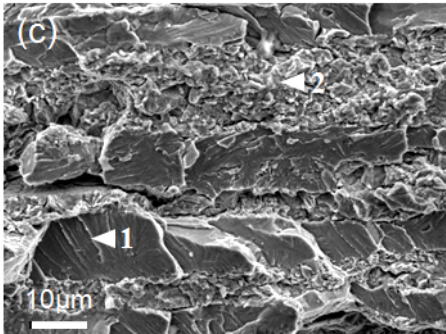
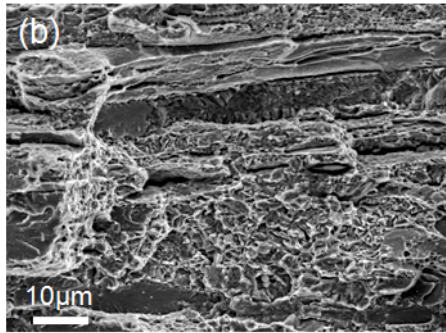
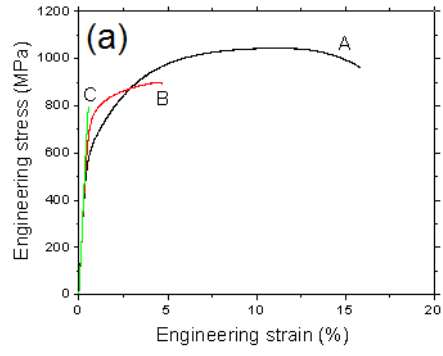


Figure 4: (a) Stress-strain curve of investigated alloys, fracture surface of (b) alloy B and (c) alloy C